Humidity Control Variable and Supersaturation

Elías Valur Hólm

ECMWF, Shinfield Park, Reading
RG2 9AX, United Kingdom
Elias.Holm@ecmwf.int

1 Introduction

All physical variables, except periodic ones like wind direction, are bound both from below and above by physical laws. Although this is most obvious for a variable like humidity, which is limited by a phase transition, other quantities like wind speed, temperature and pressure are limited by energy and mass conservation constraints. These limits are a function of the state of the physical system. A warm atmosphere can hold more water vapour before phase transitions occur than a cold one. The maximum wind inside a jetstream is limited by the available energy supply.

Let us now look at the effects on these limits on model forecasts and their errors. Assume we have an accurate, unbiased model which stays close to all the physical laws of interest. Forecast errors of an event at the limit of what is physically realizable will all fall at or below the correct value, since it should be impossible for the model to cross the limit of the realizable by design. The conditional probability distribution of the forecast errors, given that the truth is at the limits of the possible, is one-sided. Close to the physical limits, the distributions are no longer one-sided, but they are still skewed away from the limits.

As an example, consider the following humidity error behaviour. Moving from an upper tropospheric cloud to a nearby dry intrusion from the stratosphere, the humidity error drops by a factor of ten thousand. In the cloud the error distribution is almost one-sided, since any attempt at increasing humidity would just be met by condensation. In the dry intrusion the errors are severely biased towards increase in humidity, since any decrease is limited by the amount of humidity available, which is small. Close by floats a large blob of supersaturated air which mainly remains supersaturated, with the result that forecast errors are skewed towards positive values. In the vertical large gradients of humidity across the nearby tropopause add further to the inhomogeneity of the errors.

This inhomogeneous behaviour means that a detailed flow and thermodynamic state dependent description of the error pdf is needed. One way forward is to use a conditional pdf to effectively separately model different cases, giving a better knowledge of the background errors and improved description of extreme situations.

In this paper we focus on the treatment of nonlinearities in the control variable transform, including treatment of supersaturation. For further background on the humidity control variable see Hólm et al. (2002) and Dee and Da Silva (2003).

2 From physical to statistical limits

The problems we encounter close to the physical limits of the humidity concentration are signs that our assimilation model and/or its numerical representation are unphysical. The effect of the data assimilation on

the model time evolution can be seen as a source/sink S that is added to the model at the analysis time t_a, in addition to the models normal forcing R, so that the evolution of the model state x from time t_n to t_{n+1} is

$$x^{n+1} = x^n + \int_{t_n}^{t_{n+1}} (R + \delta(t - t_a)S)dt \tag{1}$$

If the assimilation term S is proportional to the field itself ($S = A(\varphi)x$, $A > 0$), the assimilation can not cause negative concentrations. If the proportionality term also includes all the conversions from humidity to condensed water and associated precipitation, humidity will never overshoot physically realistic saturation levels. However, these nonlinear processes are not easily implemented in a mainly linear assimilation framework.

An alternative approach is to statistically characterise the asymmetry of the background errors for each state of the model, which gives skewed error distributions near the physical limits of the model. These skewed distributions would only be applied at the nonlinear outer loop level of the assimilation, with the inner loops using linear approximations. Below we will study this approach further within a simple generic framework, the harmonic oscillator.

3 Illustration: Background error for a harmonic oscillator

A simple harmonic oscillator, such as a simple pendulum, oscillates with a simple harmonic motion between the maximum displacements $x = \pm A$ when slightly disturbed from the equilibrium state $x = 0$. The displacement from equilibrium for a harmonic oscillator with maximum displacement $x(t) = A$ at $t = 0$ is

$$x = A\cos\omega t \tag{2}$$

where t is time and ω is angular frequency. The error characteristics of an initial state for a harmonic oscillator (the background x^b) depend on the displacement. If the background is close to the maximum displacement, the background error probability distribution is skewed towards the equilibrium value. The most extreme case is for $x^b = \pm A$ where the distribution is one-sided. To show concrete examples of this, consider a gaussian error distributions for the angular frequency ω^b of the background,

$$P^b(\varepsilon_\omega) = \frac{1}{\sigma_\omega\sqrt{2\pi}} e^{-\frac{1}{2}(\varepsilon_\omega/\sigma_\omega)^2} \tag{3}$$

The probability distribution for the displacement background error is obtained by analytical transformations and depends on the background displacement itself, as shown in Fig. 1. As can be seen, the displacement background error has an asymmetric distribution, which makes a gaussian distribution an inaccurate model. However, when the background error is plotted as a function of both the background and the analysis, the error distribution is symmetric with respect to the axis $x^b = x^a$. We can now construct a transform that make the error distribution symmetric by replacing $P^b(\delta x|x^b)$ by $P^b(\delta x|\frac{x^b+x^a}{2})$. Since $x^a = x^b + \delta x$ this is equivalent to $P^b(\delta x|x^b + \frac{1}{2}\delta x)$. The symmetrizing transform is nonlinear, since it makes the background error model dependent not only on the background but on the analysis increments δx as well.

3.1 Symmetrizing

A practical way to construct the transform, using forecast pairs (Fisher and Andersson 2001), is as follows. Divide the forecast differences into classes according to the value of $\Phi = \frac{x_1^b+x_2^b}{2}$, where Φ will be called the stratifying variable. For each class, construct a histogram of the differences δx in order to estimate the form of the probability density function for that class. By construction, the pdf for each class is symmetric, but the shape and variance are a function of the stratifying variable Φ. In Fig. 2 we show a few of the resulting pdf's and the variance for the harmonic oscillator as a function of the stratifying variable.

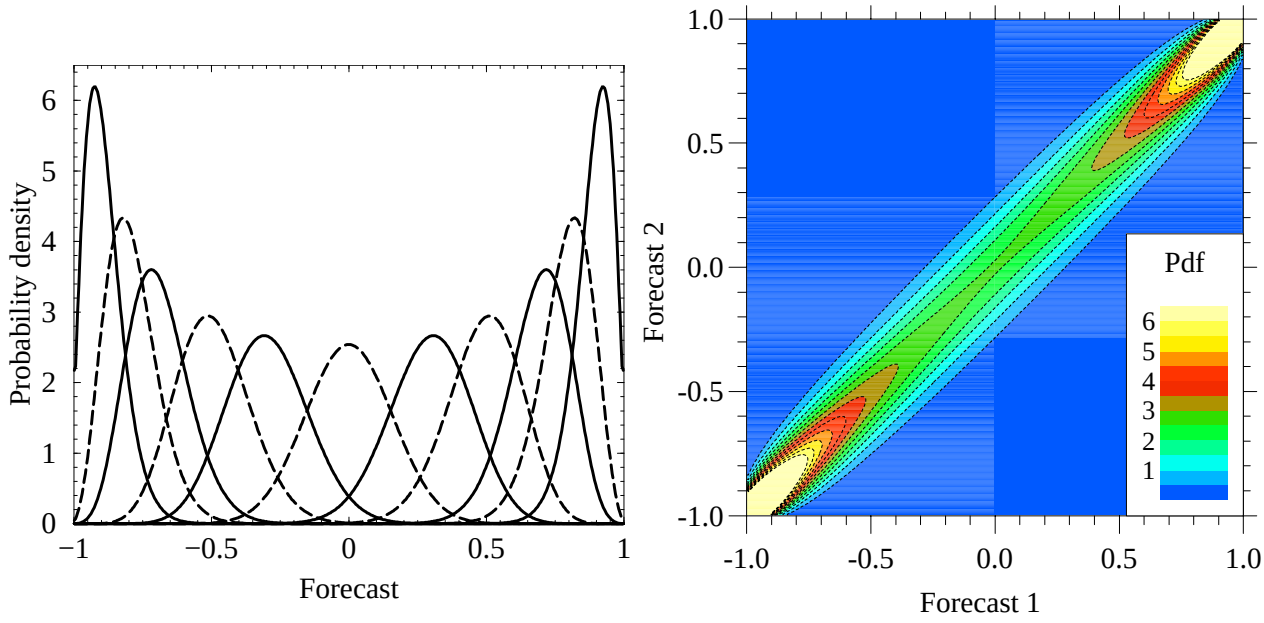

Figure 1: Probability distributions for the background error of a simple harmonic oscillator (Eq. 2 with $A = 1$; angular frequency error distribution, Eq. 3, gaussian with $\sigma_\omega = 0.1$). (a) Conditional probability $P^b(\delta x|x^b)$ for $x^b = 0, \pm 0.3, \pm 0.5, \pm 0.7, \pm 0.8, \pm 0.9$. (b) Probability as a function of background and analysis $P^b(x^b, x^a)$, $x^a =$ 'Forecast 1' and $x^b =$ 'Forecast 2'.

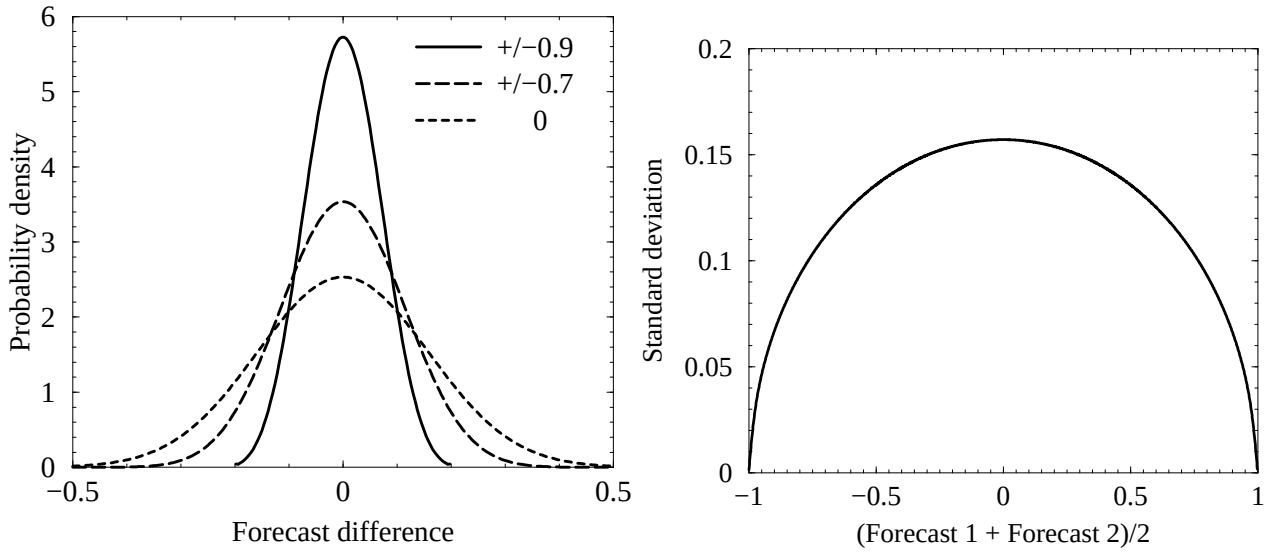

Figure 2: Symmetrized probability density functions (left) for different values of $(x_1 + x_2)/2$ and the standard deviation of the conditional pdf's (right) for all values.

3.2 Gaussianizing

These distributions turn out to be very close to a gaussian, which was established by plotting the first four moments of the distribution (not shown). For completeness, we now discuss what to do if the distribution

differs significantly from a gaussian, although we have not needed this transform when modelling humidity errors. For a given Φ, transform the δx axis by finding $f(\delta x, \Phi)$ such that the probability that $\xi \leq \delta x$ equals the probability that $\eta \leq f(\delta x, \Phi)$ for a normal gaussian distribution,

$$\Pi(\delta x|\Phi) = \int_{-\infty}^{\delta x} P(\xi|\Phi) d\xi = \int_{-\infty}^{f(\delta x,\Phi)} \frac{1}{\sqrt{2\pi}} e^{-\eta^2/2} d\eta = \Pi_G(f(\delta x, \Phi)) \tag{4}$$

where Π are the cumulative pdf's. Inverting the gaussian cumulative distribution then gives

$$f(\delta x, \Phi) = \Pi_G^{-1}(\Pi(\delta x|\Phi)) \tag{5}$$

3.3 Normalizing

Finally divide the forecast errors by $\sigma_b(\Phi)$ to get a (near) gaussian error distribution with (close to) unit variance. The complete control variable transform is then

$$\widetilde{\delta x} = \varphi(\delta x) = \frac{f(\delta x, \Phi)}{\sigma_b(\Phi)} \tag{6}$$

3.4 Implementing nonlinear analysis

The background error cost function that is being solved is nonlinear due to the nonlinearity of the control variable transform φ

$$J_b(\delta x) = \varphi^T(\delta x) B^{-1} \varphi(\delta x) \tag{7}$$

Practical implementation within a variational assimilation framework mostly requires linear inner loops, with nonlinearities collected at outer loop level. Thus the inner loops would use the linearized control variable,

$$\widetilde{\delta x} = \frac{f(\delta x, x^b)}{\sigma_b(x^b)} \tag{8}$$

In the outer loops, use the $\widetilde{\delta x}$ given by the inner loops, and solve the increment δx from the nonlinear equation

$$\frac{f(\delta x, x^b + \frac{1}{2}\delta x)}{\sigma_b(x^b + \frac{1}{2}\delta x)} - \widetilde{\delta x} = 0 \tag{9}$$

In many cases, e. g. for humidity, the above is simplified by omitting the gaussianization transform f. The nonlinear equation can be solved by e. g. Ridder's method, where one iteration may provide sufficient accuracy in our experience.

4 Supersaturated humidity background errors

Until recently significant supersaturation was not present in the ECMWF model. Cloud physics changes by Tompkins et al. (2007) changed that by modelling supersaturated water vapour with respect to mixed phase in the upper troposphere.

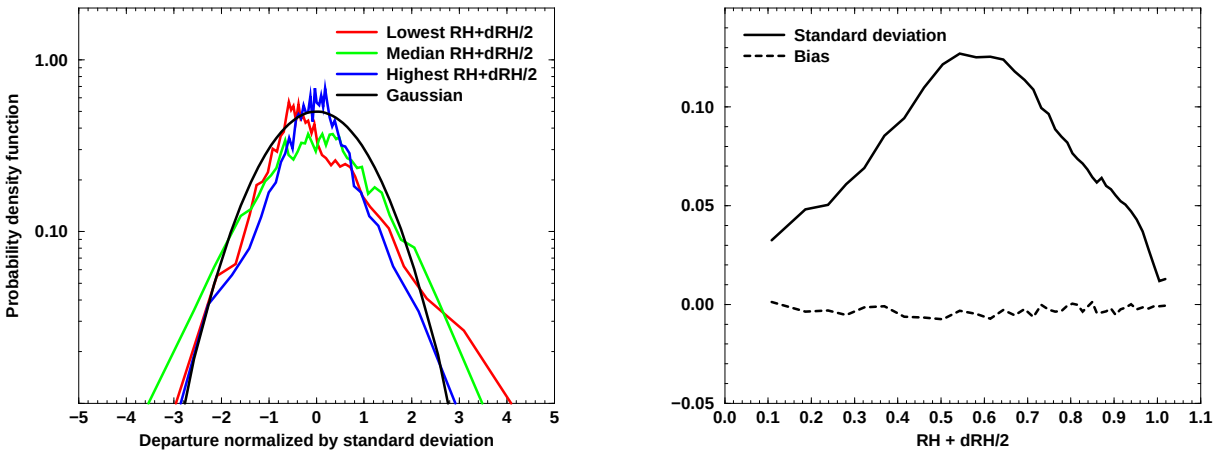

Figure 3: Forecast differences δrh at 850 hPa. The left panel shows the pdf's for lowest, median and highest 2.5% values of $rh^b + \frac{1}{2}\delta rh$, and the right panel shows the standard deviation and bias as a function of $rh^b + \frac{1}{2}\delta rh$. The pdf's compare reasonably well with the Gaussian (black line).

4.1 Characteristics of the humidity background errors

Without supersaturation, the humidity variances $\sigma(rh^b + \frac{1}{2}\delta rh)$ can be reasonably estimated by height-dependent convex functions, which go to zero at $rh^b + \frac{1}{2}\delta rh = 0$, and to low values at $rh^b + \frac{1}{2}\delta rh = 1$, with a single maxima in between (see Fig. 3). It is convenient to refer to three different regimes when discussing supersaturation, related to the ECMWF's cloud schemes interpretation of condensed water: 'warm' $T > 273K$ is pure water, mixed $273K > T > 250K$ is mixed water and ice, and $T < 250K$ is pure ice. Significant supersaturation (with respect to mixed phase) only occurs for temperatures in cold conditions below $250K$, where the cloud parameterization considers all condensed water as ice, see Fig. 4. For these conditions (e. g. upper troposphere) a second mode appears in the background errors as a function of $rh^b + \frac{1}{2}\delta rh$. The examples in this paper model the vertical variation of the nonlinear transform as a function of temperature, which in practice is not the best choice, since temperature stratification blends stratosphere and troposphere with different characteristics in each bin. This only affects the statistics at very low humidity values, but it is important to get correct limiting behaviour at low rh. Otherwise the background error can easily be overestimated by several orders of magnitude, resulting in a very bad condition number for the analysis if for example a humidity sensitive radiance is assimilated in the area. A better choice for the vertical stratification of the nonlinear transform/variances is model levels, pressure, or other coordinate monotone with respect to height.

4.2 Separate treatment of sub/supersaturated humidity

Unfortunately the nonlinear inversion which takes into account the asymmetry of the background error pdf's does not work for non-convex functions. The increments would no longer be a monotone function of the control variable, which is unphysical and can lead to multiple solutions. To cope with this, we suggest a separate treatment of supersaturated conditions. We divide the forecast differences into two classes depending on whether the background relative humidity is above or below $rh^b = 1$. If we can model the control variable for each class by a convex function, then the nonlinear transform is again viable.

Figure 5 shows warm and mixed conditions ($T > 250K$) as a function of $rh^b + \frac{1}{2}\delta rh$, separated into two classes:

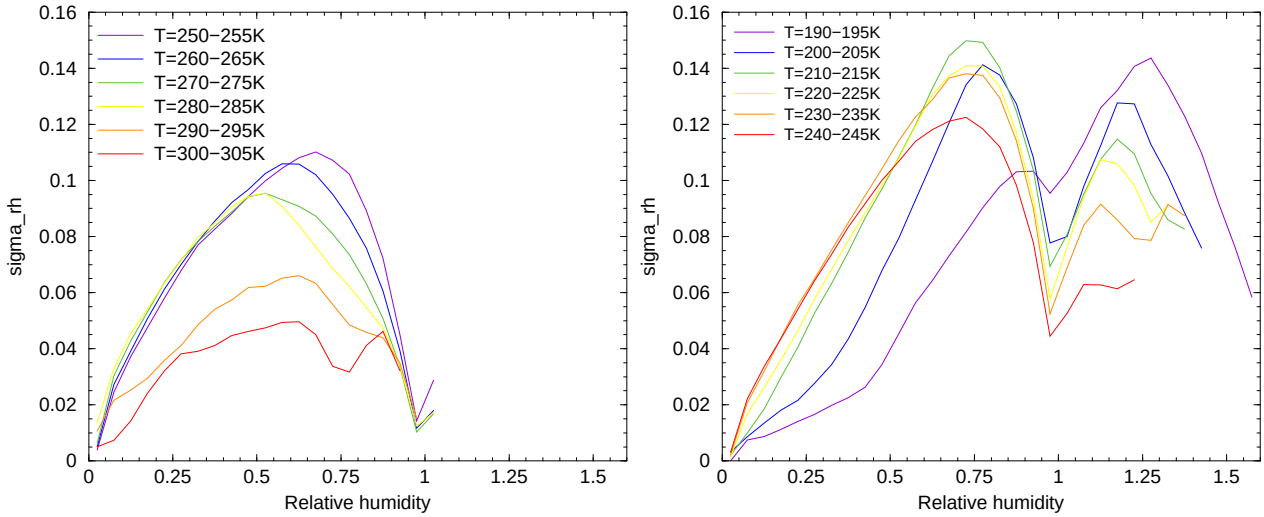

Figure 4: Background error standard deviation $\sigma_b(rh^b + \frac{1}{2}\delta rh)$ for different temperature intervals, approximately corresponding to increasing height. The left panel shows 'warm' and 'mixed' temperatures above $250K$, and the right panel shows 'cold' temperatures below $250K$, where the cloud parameterization considers all condensed water as ice.

$rh^b < 1$ (left) and $rh^b > 1$ (right). To a good degree all conditions can be modelled by a convex function, which reaches slightly into the supersaturated region, but mostly remains subsaturated. From a practical point of view, there does not seem to be any need to separate sub- and supersaturated conditions in this case. The warmest temperature range shows a double peak, related to low clouds, which can also be smoothed over by a convex approximation. For the cold conditions, Fig. 6, there are two separate distributions which each can be

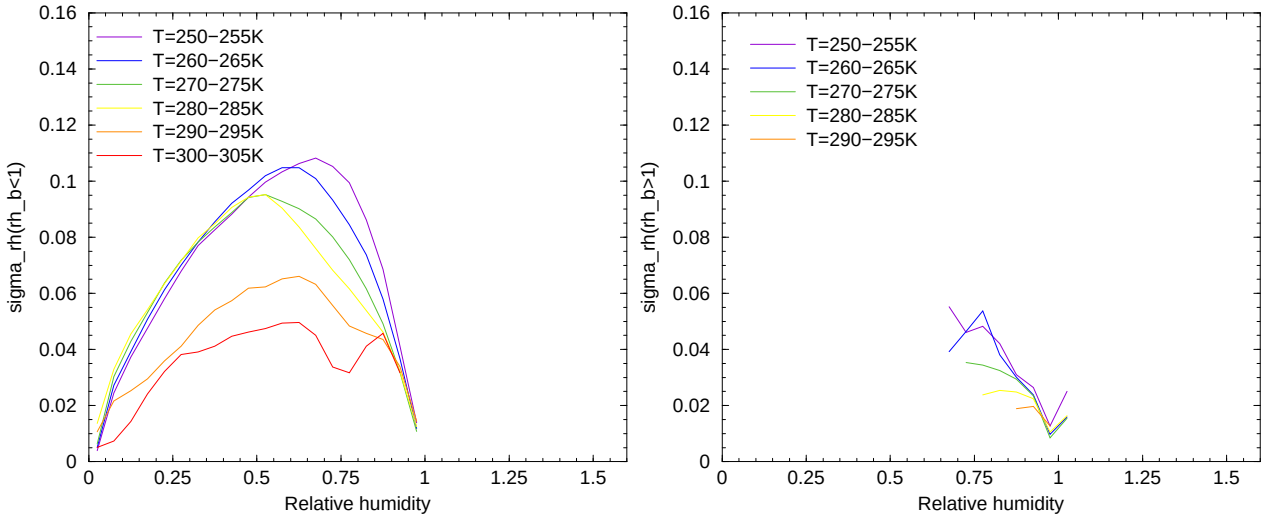

Figure 5: Background error standard deviation $\sigma_b(rh^b + \frac{1}{2}\delta rh)$ for different warm and mixed temperature intervals $T > 250K$. In the left panel $rh^b < 1$ and in the right panel $rh^b > 1$.

modelled by a convex function, again smoothing over any dips, e. g. at $rh \approx 1$, with reasonable accuracy. In Fig. 7 we look more closely at how the analysis moves between sub- and supersaturated regions.

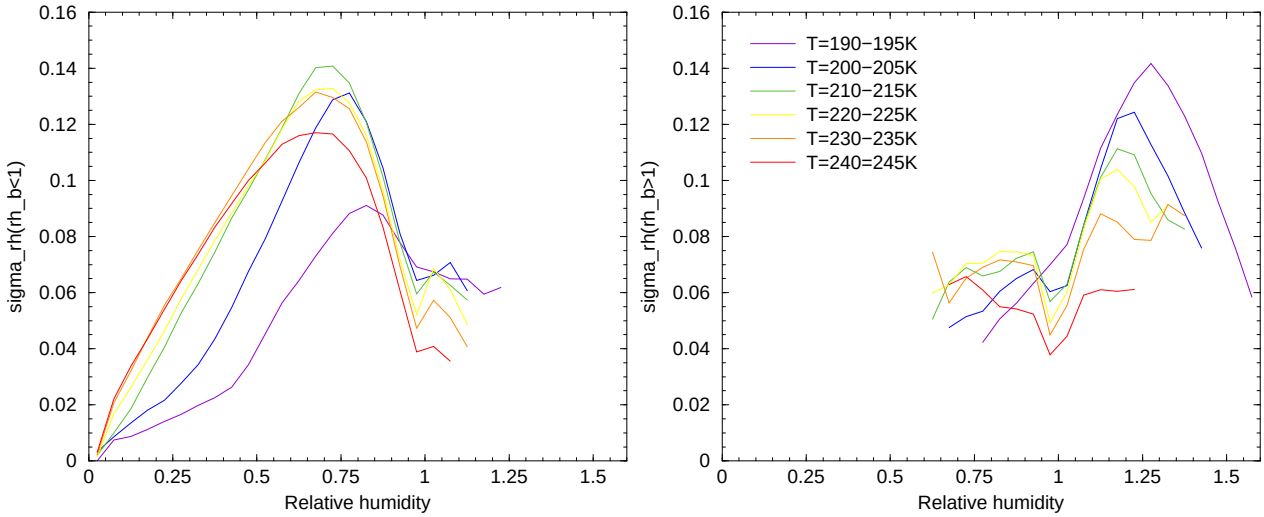

Figure 6: Background error standard deviation $\sigma_b(rh^b + \frac{1}{2}\delta rh)$ for different cold temperature intervals $T < 250K$. In the left panel $rh^b < 1$ and in the right panel $rh^b > 1$.

For warm conditions (right) both background and analysis predominantly remain below saturation, with the analysis at most reaching a few percent supersaturation. Above it was concluded that the background error pdf can be modelled by a single convex pdf in this case, and Fig. 7 shows that this pdf needs to include a couple of percent supersaturation, allowing transition into slight supersaturation.

For cold conditions (left), there is a significant proportion of moist points which change from sub- to supersaturated conditions and vice versa. If we model the pdf of background errors by two separate convex conditional distributions as suggested above, one for $rh^b < 1$ and the other for $rh^b > 1$, Fig. 7 shows the range necessary for the two distributions. For this particular temperature range, the pdf for $rh^b < 1$ can go up to $\frac{1}{2}(rh^b + rh^a) \approx 1.2$, i. e. $rh^a < 1.4$. This allows for a transition from sub- to supersaturated conditions. The pdf for rh^b can go down to $\frac{1}{2}(rh^b + rh^a) \approx 0.7$, i. e. $rh^a > 0.4$, allowing super- to subsaturated transition.

At each outer loop iteration the choice of conditional pdf is determined by the value of the nonlinear trajectory, thus allowing for different choice on different iterations as needed. It should be noted finally that the splitting of the pdf into two as a function of rh^b does reintroduce some asymmetry in the conditional pdf's close to saturation. But that disadvantage is hopefully balanced by the simplified description of the nonlinear error behaviour close to saturation.

5 Conclusions

Variables limited by upper and lower physical bounds, like humidity, have asymmetric background errors close to these limits. A nonlinear transform, which symmetrizes the error pdf's, can be applied at outer loop level in the assimilation to address this. The extension of this nonlinear transform to supersaturated conditions is not trivial, since the supersaturation produces a second mode in the error statistics. The nonlinear transform must be convex for the increments to be a monotone function of the control variable, but this is impossible for a function with two maxima. A pragmatic solution is to treat the error statistics of the two modes separately, which gives two convex functions and enables a separate nonlinear transform for each case.

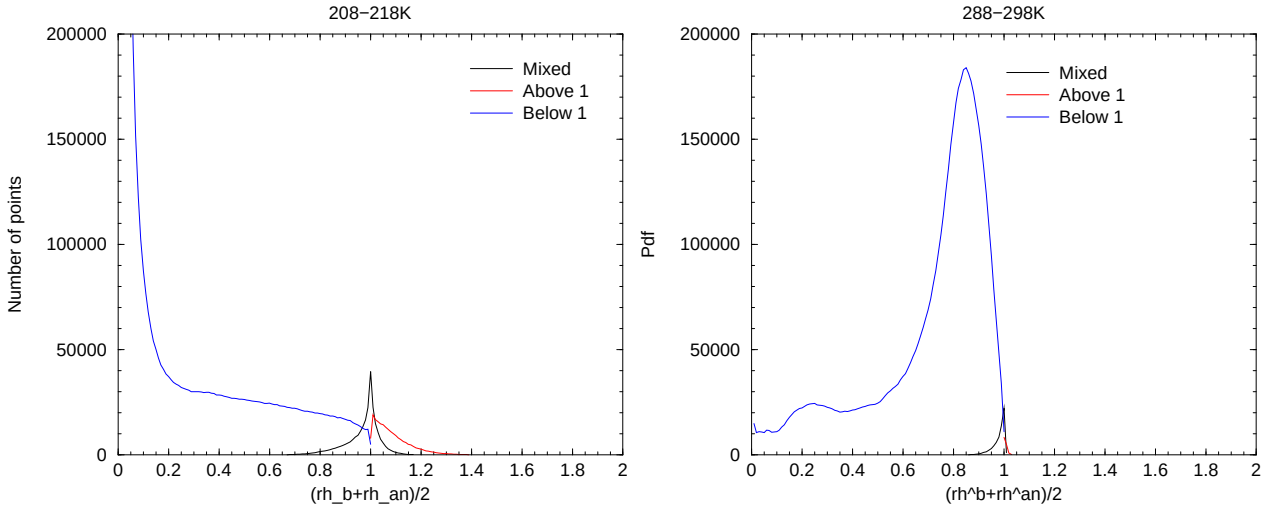

Figure 7: Pdf's of $rh^b + \frac{1}{2}\delta rh$ for a cold (left) and warm (right) temperature range. Each plot shows three distributions: $rh^b < 1$ and $rh^a < 1$ (blue); $rh^b > 1$ and $rh^a > 1$ (red); $rh^b < 1$, $rh^a > 1$ or $rh^b > 1$, $rh^a < 1$ (black).

References

[1] Dee, D. P., and A. M. Da Silva, 2003: The Choice of Variable for Atmospheric Moisture Analysis. *Mon. Wea. Rev.*, **131**, 155–171.

[2] Fisher, M. and E. Andersson, 2001: *Developments in 4D-Var and Kalman Filtering.* ECMWF Research Department Technical Memorandum **347**.

[3] Hólm, E., E. Andersson, A. Beljaars, P. Lopez, J.-F. Mahfouf, A. Simmons and J.-N. Thépaut, 2002: *Assimilation and Modelling of the Hydrological Cycle: ECMWF's Status and Plans.* ECMWF Research Department Technical Memorandum **383**.

[4] Tompkins, A. M., K. Gierens, and G. Rädel, 2007: Ice supersaturation in the ECMWF integrated forecast system. *Q. J. R. Meteorol. Soc.*, **133** 53–63